[Article] Steady Combustion Waves Driven by a Recombination Reaction in a Gas Mixture

Steady Combustion Waves Driven by a Recombination Reaction in a Gas Mixture

Fiammetta Conforto ·Maria Groppi · Roberto Monaco ·Giampiero Spiga

Abstract Steady combustion waves in one space dimension are studied by means of fluiddynamic reactive Navier–Stokes equations derived from kinetic theory. By using the conservation laws, the problem is reduced to a three-dimensional dynamical system, with different solutions of deflagration or detonation type according to several various sub-regions in the parameter space. The delicate question of the flame eigenvalue is addressed, and a suitable numerical algorithm is used in order to catch these special solutions and to deal with the relevant unstable equilibrium states. Numerical examples of smooth weak deflagrations or detonations are shown.

Keywords Kinetic theory · Chemical reactions · Combustion waves

Mathematics Subject Classification 82C40 · 80A25 · 76V05

1 Introduction

The combustion processes are of great interest from the experimental, theoretical and computational point of view for their crucial role in the energy production and have been widely studied in the last fifty years [7, 8, 11].

F. Conforto ()
Dept. of Mathematics, Università di Messina, Viale F. Stagno d'Alcontres 31, 98166 Messina, Italy e-mail: fiammetta.conforto@unime.it

M. Groppi · G. Spiga

Dept. of Mathematics, Università di Parma, Parco Area delle Scienze 53/A, 43124 Parma, Italy

M. Groppi
e-mail: maria.groppi@unipr.it

G. Spiga e-mail: giampiero.spiga@unipr.it

R. Monaco
Dept. of Regional and Urban Studies and Planning, Politecnico di Torino, Corso Duca degli Abruzzi 24,
10129 Turin, Italy
e-mail: roberto.monaco@polito.it

The combustion is characterized by many and different factors (see [11] and related bibliography), like for instance the time and space dependence, the mixing conditions and the phases in the initial state, as well as the rates of the chemical processes and the wave speed. In fact, two relevant combustion phenomena, as detonation and deflagration, are fundamentally distinguished by their speed of propagation: the former moves with supersonic speed, the latter propagates with subsonic speed.

There are many strong assumptions usually made in combustion modeling [11]: infinitely fast chemistry, the reacting fluid treated as a continuum, simple one step irreversible reactions, Fick's law of diffusion, uniform pressure in deflagration regime, equal mass diffusivities, ideal gas law, Lewis, Schmidt and Prandtl number equal to one, negligible Dufour and Soret effects. In addition, numerical comparison with experimental data, which are mainly concerned with measurement of the wavefront speed, is seldom possible, also because of the difficulties of reproducing in a laboratory the idealized physical situations underlying theoretical models.

In the authors' opinion, the accuracy of the theoretical description of the physical peculiarities and of chemical reactions has a basic importance for reliability, prediction capability and simulation of the whole process. For this reason, in a previous paper [5], at least some of the various simplifications above have been removed, starting from a set of reactive Boltzmann equations at the kinetic level [3], deducing consistently by a Chapman–Enskog expansion the macroscopic governing equations [4], and achieving, by an accurate description of the chemical interactions, explicit expressions of the reaction rates. The effort was aimed at improving the more usual modeling based on standard or extended thermodynamics [12, 13]. In particular, in [5] the more realistic irreversible exothermic recombination reaction of two atoms in a diatomic molecule passing through an excited unstable state has been considered, i.e. $A \quad A \quad A_2^{exc} \quad A_2$ [9+ → →]. This reaction is significant for applications, and represents a kind of nontrivial intermediate level between the simplest one-way reactions A → B mainly used in literature, on one side, and the complex reaction chains involved in experimental setups, on the other. The resulting exact set of balance laws was then closed by resorting to specific constitutive equations for heat flux and diffusion velocities derived for a binary mixture of hard spheres, though ignoring, as quite common [6, 7, 11], viscosity and thermal diffusion. There is no doubt that it would be interesting to take into account these dissipative effects in the various physical scenarios. Although viscosity, as well as other simplifying assumptions, may play a non-negligible role, at this step we still prefer to handle a model ensuring simplicity and consistency at the same time. However, the matter will hopefully be subject of future investigation; inclusion of the viscous stress should be matter of some technicality (in our setting, it amounts to increasing by one the dimension of the resulting dynamical system), whereas consideration of Soret and Dufour effects on mass and thermal diffusion, or of more realistic reaction chains, even in higher space dimensions, will constitute more delicate tasks.

In the above article [5], theoretical results were illustrated by some numerical examples of steady propagation of deflagration waves in a particular regime. In this paper, in the same framework of [5], a more systematic classification and analysis, along the lines which are more common in the theory of combustion, of all possible steady solutions is presented. In detail, all the deflagration and detonation regimes are deduced in one dimension in Sect. 2. Such propagation occurs in the direction of the negative x-axis at a constant speed towards the unburned gas which is at rest in metastable equilibrium. The burned gas, following the wave front, is in thermodynamical equilibrium and moves also to the left at constant speed; the problem is then studied in the wave reference frame, so that governing equations become stationary.

In Sect. 3 the combustion problem is represented, as usual in the literature, by the Hugoniot diagram. As well-known [11], the combustion states lie, in the pressure versus specific volume plane, at the intersections between the Rayleigh lines (all passing through the unburned state and whose slope varies with the unburned Mach number) and the Hugoniot curves, whose equations are deduced by the conservation laws of mass, momentum and energy. The Hugoniot hyperbolae form a sheaf parameterized by a quantity describing the progress of the chemical reaction from the unburned to the burned equilibrium state; since the reaction is exothermic, the hyperbola of the equilibrium states is the farthest from the axes. Each hyperbola is divided into two branches, separated by an intermediate un-physical region: the detonation branch for low specific volume and high pressure, and the deflagration one for high specific volume and low pressure. The tangency points between the Rayleigh lines and the equilibrium Hugoniot hyperbola, the so-called upper Chapman–Jouguet (C–J) point U on the detonation branch and lower C–J point L on the deflagration one, play a crucial role: in fact, they provide, for the slope of the Rayleigh lines, the lower and upper bounds for which detonation and deflagration solutions occur, respectively. Of course, it is shown that a quantitative analysis of the Hugoniot diagram yields the same results on existence and physical features of steady combustion waves in the parameter space as the direct investigation performed in Sect. 2 of [5].

Finally, Sect. 4 is devoted to the numerical determination of smooth steady deflagration and detonation profiles by means of the considered balance equations and hydrodynamic closures. The problem is delicate, since existence of such profiles is well known to request a very precise balance of gas inflow, reaction rate, and thermal conductivity. This is what occurred for deflagration in [12], and what is in order also for detonation in our Navier-Stokes approach. In fact, there exists in our balance laws a dissipative mechanism (specifically, heat conduction) to oppose the exothermic reactive heat release, so that our process can be classified, according to the pertinent literature [2, 6], as an “eigenvalue detonation”, where the propagation velocity of the steady wave must be eigenvalue of the governing set of differential equations, and depends on the details of both reaction rates and state equation. This is in sharp contrast to the standard Chapman–Jouguet detonation, which can be adequately described at the Euler level, and where such a constraint does not exist. An additional difficulty is that the numerical algorithm for the solution of the balance equations is uneasy, since burned states are always unstable equilibria for the dynamical system, and one has to integrate backwards, starting from a neighborhood of the downstream equilibrium, and looking for the unburned state upstream. Some plots of wave profiles and Hugoniot diagrams are shown for both deflagration and detonation.

2 The Steady 1-D Combustion Problem

In paper [5], for the reacting mixture under investigation, the governing equations for the state variables c, n, u, T , J, q, in one space dimension, has been derived and read

$$\frac{d}{dx}(cnu + J) = -2S, \tag{1}$$

$$\frac{d}{dx}\left[(2-c)nu\right] = 0, \tag{2}$$

$$\frac{d}{dx}\left[m(2-c)nu^2 + nKT\right] = 0, \tag{3}$$

$$\frac{d}{dx}\left[\frac{1}{2}m(2-c)nu^3 + \frac{5}{2}nKTu - E_0(1-c)nu + \frac{E_0}{2}J + q\right] = 0, \tag{4}$$

where n is the total number density, c the atom concentration (ratio of atom number density to n), u the mean velocity of the whole mixture, T the temperature, J the diffusion flux of atoms, and q the heat flux. Moreover, m is the atom mass, K the Boltzmann constant, $E_0 > 0$ the energy of chemical link of the molecule, D_{12} the diffusion coefficient of atoms into molecules and λ the thermal conductivity. The total mass density is given by ρ = m(2 − c)n and the mixture obeys the equation of state of perfect gases p = nKT . The last two equations (5) and (6) are the constitutive equations proposed in [14, 15]. Finally, the chemical production term S is given by

$$S = \frac{2k}{\sqrt{\pi}}c^2n^2\Gamma\left(\frac{3}{2}, \frac{A}{KT}\right), \tag{7}$$

where k is the reaction strength, A the activation energy and Γ an incomplete Euler gamma function [1].

In what follows we refer to the framework of combustion propagation, that is we are looking for a wave profile starting from the unburned gas state

$$c = 1, \qquad n = n_0 > 0, \qquad u = u_0 > 0, \qquad T = T_0 > 0, \qquad J = 0, \qquad q = 0, \tag{8}$$

which is in metastable equilibrium, i.e. A KT_0.

For convenience, dimensionless variables are now introduced through the following rescaling

$$\frac{n}{n_0} \to n, \qquad \frac{u}{u_0} \to u, \qquad \frac{T}{T_0} \to T, \qquad \frac{J}{n_0u_0} \to J, \qquad \frac{q}{mn_0u_0^3} \to q,$$

$$x\frac{Kn_0u_0}{\lambda\sqrt{T_0}} \to x, \qquad \frac{E_0}{KT_0} \to E_0. \tag{9}$$

By following the procedure of [5], Eqs. (1), (5), (6) are rewritten as follows in terms of the field variables (c,u,J)

$$\begin{aligned}
\frac{dc}{dx} &= -\frac{L}{2}(2-c)\frac{J}{\sqrt{T}} \\
\frac{du}{dx} &= \frac{1}{(2-c)\sqrt{T}}\left(1 + \frac{5}{3}M_0^2 - \frac{10}{3}M_0^2u\right)^{-1} \\
&\quad \times\left\{-E_0\frac{1-c}{2-c} + \frac{J}{2}\left[E_0 - L(2-c)\left(1 + \frac{5}{3}M_0^2 - \frac{5}{3}M_0^2u\right)u\right]\right. \\
&\quad \left. + \frac{5}{6}M_0^2(u^2-1) + \frac{5}{2}(u-1)\left(1 - \frac{5}{3}M_0^2u\right)\right\} \\
\frac{dJ}{dx} &= L\frac{J}{(2-c)\sqrt{T}} - \frac{4\mu}{\sqrt{\pi}}\frac{c^2}{(2-c)^2u^2}\Gamma\left(\frac{3}{2}, \frac{T_{act}}{T}\right),
\end{aligned} \tag{10}$$

where the remaining variables have been determined in terms of (c,u,J) through the conservation laws

$$n = \frac{1}{(2-c)u}, \tag{11}$$

$$T = (2-c)\left[\left(1+\frac{5}{3}M_0^2\right)u - \frac{5}{3}M_0^2u^2\right], \tag{12}$$

$$q = \frac{1}{2} + \frac{3}{2M_0^2} + 2u^2 - \left(\frac{5}{2} + \frac{3}{2M_0^2}\right)u + \frac{3E_0}{5M_0^2}\left(\frac{1-c}{2} - \frac{J}{2}\right). \tag{13}$$

The Lewis number L, the activation temperature T_{act}, the flame eigenvalue μ [12] and the Mach number M_0 relative to the unburned state are given by

$$L = \frac{\lambda}{K D_{12}}, \qquad T_{act} = \frac{A}{K T_0}, \qquad \mu = \frac{\lambda k\sqrt{T_0}}{K u_0^2}, \qquad M_0^2 = \frac{3mu_0^2}{5KT_0}. \tag{14}$$

Notice that T_{act} measures the activation energy in units of a mean thermal energy in the unburned state, so that metastability of such a state is guaranteed if $T_{act} \gg 1$. In fact, if this is the case, the chemical reaction is strongly inhibited, and essentially does not occur on the considered physical scales.

From the dynamical system (10) it is evident that u blows up at the following critical value

$$u_{crit} \equiv \frac{1}{2}\left(1 + \frac{3}{5M_0^2}\right). \tag{15}$$

Moreover from (11) and (12) it follows that $n > 0 \Rightarrow u > 0$, and

$$T > 0 \quad \Rightarrow \quad 0 < u < u_{max} := 1 + \frac{3}{5M_0^2} = 2u_{crit}.$$

The subsonic and supersonic regimes are respectively characterized by $u < u_s$ and $u > u_s$, where

$$u_s = \frac{5}{8} + \frac{3}{8M_0^2} = \frac{5}{8}u_{max} = \frac{5}{4}u_{crit}. \tag{16}$$

The steady combustion wave connects the unburned gas upstream to the burned equilibrium state downstream. Consequently, we search the equilibria of the dynamical system (10) finding the following two points

$$u_{eq}^{\pm} = \frac{3}{8M_0^2}\left[1 + \frac{5}{3}M_0^2 \pm \sqrt{\left(M_0^2-1\right)^2 - \frac{16}{15}E_0M_0^2}\right], \qquad c_{eq} = 0, \qquad J_{eq} = 0, \tag{17}$$

which exist only if the parameter M_0 satisfies the inequalities

$$M_0^2 \le M_{eq}^- < 1 \quad \text{or} \quad M_0^2 \ge M_{eq}^+ > 1, \tag{18}$$

$$M_{eq}^{\pm} = 1 + \frac{8}{15}E_0 \pm \sqrt{\frac{64}{225}E_0^2 + \frac{16}{15}E_0}. \tag{19}$$

When $M_0^2 = M_{eq}^-$ or $M_0^2 = M_{eq}^+$, a unique equilibrium state

$$u_{eq} = u_s, \qquad c_{eq} = 0, \qquad J_{eq} = 0, \tag{20}$$

is obtained. In all cases, downstream burned equilibria are defined by

$$c = 0, \qquad n = n_{eq}, \qquad u = u_{eq}, \qquad T = T_{eq}, \qquad J = 0, \qquad q = 0, \tag{21}$$

where n_{eq} and T_{eq} are computed through (11) and (12) for $c = 0$ and $u = u_{eq}$.

We are interested in deriving the order relations between the quantities $u^{\pm}_{eq}$, u_s, u_{crit}, u_{max} and the unburned state characterized by u = 1. We set

$$M_1 = \frac{3}{5(3+E_0)}, \qquad M_2^{\pm} = \frac{3}{5}\left(2 + E_0 \pm \sqrt{1+4E_0+E_0^2}\right), \tag{22}$$

obeying

$$M_1 < M_{2^-} < M_{eq^-} < 1 \quad \text{and} \quad 1 < M_{eq^+} < M_{2^+}. \tag{23}$$

The order relations can be summarized in the following statements

- $u^-_{eq} \le u_s \le u^+_{eq}\ \forall M_0^2 \le M^-_{eq}$ or $\forall M_0^2 \ge M^+_{eq}$
- $u_{crit} < u_s < u_{max}\ \forall M_0^2 \le M^-_{eq}$ or $\forall M_0^2 \ge M^+_{eq}$
- $u_{+eq} > u_{crit}\ \forall M_{02} \le M_{eq^-}$ or $\forall M_{02} \ge M_{eq^+}$
- $u_s < 1 \Leftrightarrow M_0^2 > 1$
- $u^{\pm}_{eq} < 1 \Leftrightarrow M_0^2 > 1$
- $u_{+eq} < u_{max} \Leftrightarrow M_0^2 > M_{1_{max}}$
- $u_{-eq} < u_{crit} \Leftrightarrow M_0^2 < M_2^- < 1$ or $M_0^2 > M_2^+ > 1$
- $u_{crit} < 1 \Leftrightarrow M_0^2 > 3/5$
- $M^-_{eq} < \frac{3}{5} \Leftrightarrow E_0 > \frac{1}{4}$

For what concerns the stability analysis of the dynamical system (10), the associated Jacobian matrix in the equilibrium state $(0,u^{\pm}_{eq},0)$, after some algebra, exhibits three real eigenvalues given by

$$\lambda_1 = 0, \qquad \lambda_2 = \frac{L}{2\sqrt{T^{\pm}_{eq}}}, \qquad \lambda_3 = \mp \frac{5\sqrt{(M_0^2-1)^2 - \frac{16}{15}E_0 M_0^2}}{4(1+\frac{5}{3}M_0^2 - \frac{10}{3}M_0^2 u^{\pm}_{eq})\sqrt{T^{\pm}_{eq}}}, \tag{24}$$

where

$$T^{\pm}_{eq} = 2\left(1 + \frac{5}{3}M_0^2 - \frac{5}{3}M_0^2 u^{\pm}_{eq}\right)u^{\pm}_{eq}$$

is the dimensionless temperature (12) evaluated at the equilibrium $(0,u^{\pm}_{eq},0)$. Thus, because of λ_2, equilibria are all unstable, and, because of λ_1, a central manifold always exists [10]. Concerning the sign of the third eigenvalue it is easy to check that $\lambda_3|_{u=u_{-eq}} > 0$ iff $u^-_{eq} < u_{crit}$ and $\lambda_3|_{u=u_{+eq}} > 0$ iff $u^+_{eq} > u_{crit}$, and that in such cases the unstable manifold is two-dimensional.

We are now able to give a complete list of the possible steady combustion waves, and of their type, in the different ranges of the various physical parameters.

2.1 Deflagrations

Deflagrations occur when $M_0^2 < 1$, and we get two different families of admissible results depending on the values of E_0. In detail

1. if $E_0 > 1/4$, then $M_1 < M_2^- < M_{eq}^- < 3/5$. In this case such a family exhibits three different possible deflagration regimes
   (a) if $M_0^2 \leq M_1$, then $1 < u_{eq}^- < u_{crit} < u_s < u_{max} \leq u_{eq}^+$ and the solution consists in a weak smooth deflagration connecting the states (1,1,0) and $(0,u_{eq}^-,0)$, with $\lambda_3 > 0$;
   (b) if $M_1 < M_0^2 \leq M_2^-$, then $1 < u_{eq}^- \leq u_{crit} < u_s < u_{eq}^+ < u_{max}$ and this time we get again a weak smooth deflagration from (1,1,0) to $(0,u_{eq}^-,0)$ with $\lambda_3 > 0$, or a strong deflagration from (1,1,0) to $(0,u_{eq}^+,0)$, with a jump discontinuity and with $\lambda_3 > 0$;
   (c) if $M_2^- < M_0^2 \leq M_{eq}^-$, then $1 < u_{crit} < u_{eq}^- \leq u_s \leq u_{eq}^+ < u_{max}$ and the solution is now a weak deflagration from (1,1,0) to $(0,u_{eq}^-,0)$ with a jump discontinuity and with $\lambda_3 < 0$, or a discontinuous strong deflagration from (1,1,0) to $(0,u_{eq}^+,0)$, with $\lambda_3 > 0$.
2. if $E_0 \leq 1/4$, then $M_1 < M_2^- < 3/5 \leq M_{eq}^-$. In this case four different deflagration regimes may occur
   (a) if $M_0^2 \leq M_1$, then $1 < u_{eq}^- < u_{crit} < u_s < u_{max} \leq u_{eq}^+$ and the solution consists in a weak smooth deflagration connecting the states (1,1,0) and $(0,u_{eq}^-,0)$ with $\lambda_3 > 0$, analogously to the result of the first family;
   (b) if $M_1 < M_0^2 \leq M_2^-$, then $1 < u_{eq}^- \leq u_{crit} < u_s < u_{eq}^+ < u_{max}$ and we get again a weak smooth deflagration from (1,1,0) to $(0,u_{eq}^-,0)$ with $\lambda_3 > 0$, or a discontinuous strong deflagration from (1,1,0) to $(0,u_{eq}^+,0)$, with $\lambda_3 > 0$;
   (c) if $M_2^- < M_0^2 \leq 3/5$, then $1 \leq u_{crit} < u_{eq}^- < u_s < u_{eq}^+ < u_{max}$ and now a discontinuous weak deflagration from (1,1,0) to $(0,u_{eq}^-,0)$ with $\lambda_3 < 0$, or a discontinuous strong deflagration from (1,1,0) to $(0,u_{eq}^+,0)$ with $\lambda_3 > 0$ is obtained;
   (d) if $3/5 < M_0^2 \leq M_{eq}^-$, then $u_{crit} < 1 < u_{eq}^- \leq u_s \leq u_{eq}^+ < u_{max}$ and finally we get a weak smooth deflagration between the states (1,1,0) and $(0,u_{eq}^-,0)$ with $\lambda_3 < 0$, or a smooth strong deflagration from (1,1,0) to $(0,u_{eq}^+,0)$, with $\lambda_3 > 0$.

In this case, however, one should bear in mind that, for physical reasons, strong deflagration solutions do not exist (and, in fact, are never observed experimentally in a one space dimension setup, since a change from subsonic to supersonic flow can never occur in a constant area duct [11]), and therefore all such mathematically plausible waves (either smooth or discontinuous), which might connect the states (1,1,0) and $(0,u_{eq}^+,0)$, must be discarded. This leaves a unique physically observable solution in each allowed range of the parameter space.

2.2 Detonations

We turn our attention to the ranges of M_0, such that $M_0^2 \geq M_{eq}^+ > 1$, allowing detonation profiles. In this regime, $1 < M_{eq}^+ < M_2^+$, $\forall E_0$. Specifically, this family exhibits two different kinds of possible regimes.

1. if $M_{eq}^+ \leq M_0^2 < M_2^+$, then $u_{crit} < u_{eq}^- \leq u_s \leq u_{eq}^+ < 1 < u_{max}$ and we have a weak smooth

detonation solution connecting (1,1,0) to $(0,u^{+}_{eq},0)$, with $\lambda_3 > 0$, or a strong smooth detonation between the states (1,1,0) and $(0,u^{-}_{eq},0)$, with $\lambda_3 < 0$;

2. if $M_0^2 \geq M_2^+$, then $u^{-}_{eq} \leq u_{crit} < u_s < u^{+}_{eq} < 1 < u_{max}$ and we get again a weak smooth detonation from (1,1,0) to $(0,u^{+}_{eq},0)$, with $\lambda_3 > 0$, or a strong discontinuous detonation between the states (1,1,0) and $(0,u^{-}_{eq},0)$, with $\lambda_3 > 0$.

In this case one should remember again that eigenvalue detonations are characterized by a supersonic final equilibrium state [6], so that all possible mathematically admissible strong detonations connecting the states (1,1,0) and $(0,u^{-}_{eq},0)$ must be excluded for physical reasons. Once more, this leaves a unique observable solution in each range of the parameter space.

3 The Hugoniot Diagram

As already discussed in the Introduction, combustion problems are well described by the socalled Hugoniot diagram [11] which represents the processes on the pressure versus specific volume plane. Of course, in this representation, one should bear in mind that such a plane does not exhaust the phase space for the dynamical system (10), which is three-dimensional, so that a third coordinate, independent of pressure p and specific volume v, is needed to define the point describing the evolution of the gas mixture. For our purposes it is convenient to re-write the conservation laws (2)–(4) in terms of

$$\frac{d}{dx}\left[(2-c)nu\right] = 0$$

$$\frac{d}{dx}\left[\frac{5}{3}M_0^2(2-c)nu^2 + nT\right] = 0,$$

$$\frac{d}{dx}\left[\frac{5}{6}M_0^2(2-c)nu^3 + \frac{5}{2}nTu - E_0(1-c)nu + \frac{E_0}{2}J + \frac{5}{3}M_0^2 q\right] = 0.$$

dimensionless variables, introducing M_0^2 as well. After some algebra they read

, (25)

(26)

(27)

When integrating between the unburned and the general state, integration constants are determined by the unburned state itself, and, using the dimensionless mass density ρ = (2 − c)n and pressure p = nT into the conservation equations of mass (25) and momentum (26), we get respectively,

$$v = \frac{1}{\rho} = u, \qquad p - 1 = \frac{5}{3}M_0^2\left(1 - \frac{u^2}{v}\right), \tag{28}$$

where v denotes the specific volume. Eliminating u yields the Rayleigh line equation

$$p-1=-\frac{5}{3}M_0^2(v-1), \tag{29}$$

which represents the projection on the (v,p) plane of the actual phase trajectory. Then, from the conservation equation of energy (27) we get

$$\frac{5}{6}M_0^2(2-c)nu^3+\frac{5}{2}pu-E_0(1-c)nu+\frac{E_0}{2}J+\frac{5}{3}M_0^2q=\frac{5}{6}M_0^2+\frac{5}{2} \tag{30}$$

which, combined together with (28), leads to the Hugoniot curve equation (31)

$$\frac{5}{2}(vp-1)-\frac{1}{2}(p-1)(v+1)=Q\equiv E_0\frac{1-c}{2\quad c}-\frac{E_0}{2}J-\frac{5}{3}M_0^2q, \tag{31}$$

where Q is a quantity depending on the fields (c,J,q) which evolves versus x as the combustion proceeds. In fact, using (11)–(13), Q may be cast in terms of the unknowns of the dynamical system (10), and can then be evaluated at any given step of the reaction. In particular, there results that Q depends on x only through the variable u, Q = Q[u(x)], where

$$Q(u)=-\frac{10}{3}M_0^2u^2+\left(\frac{25}{6}M_0^2+\frac{5}{2}\right)u-\frac{5}{6}M_0^2-\frac{5}{2} \tag{32}$$

is easily seen to be monotonically increasing or decreasing according to whether $u < u_s$ or $u > u_s$.

It is convenient to re-write the Hugoniot curve in the following form

$$\left(p+\frac{1}{4}\right)\left(v-\frac{1}{4}\right)=\frac{Q}{2}+\frac{15}{16}. \tag{33}$$

These curves are hyperbolae, and their physical branch is relevant to the restriction Q > −15/8 (first quadrant). For Q = −15/8 the hyperbola degenerates into its two asymptotes, p = −1/4 and v = 1/4.

As well-known, all the possible combustion states lie at the intersection between a Rayleigh line, characterized by a fixed value of the Mach number M_0, and a Hugoniot curve, parameterized by M_0 itself and by a value of Q, which identifies an intermediate state of the whole chemical process. The parameter Q in the unburned state assumes the value $Q_0 = Q(1,0,0) = 0$, whereas in the burned one is equal to $Q_{eq} = Q(0,0,0) = E_0/2 > 0$.

Existence of a combustion solution on the Hugoniot diagram consists in finding the intersections between the Rayleigh lines and the whole Hugoniot sheaf, yielding, for fixed given values of M_0^2 and Q, the following equation for v

$$\frac{5}{3}M_0^2v^2-\frac{5}{4}\left(1+\frac{5}{3}M_0^2\right)v+\frac{5}{4}+\frac{5}{12}M_0^2+\frac{Q}{2}=0. \tag{34}$$

Since the inhomogeneous term is always positive for Q > −15/8, real and positive solutions are obtained if, for each given M_0^2,

$$Q\le\frac{15}{32}\frac{(M_0^2-1)^2}{M_0^2}\equiv Q_s, \tag{35}$$

where Q_s parametrizes the hyperbola which is tangent to the Rayleigh line.

The two C–J points, which provide for the Mach number M_0 the lower bound for detonation and the upper bound for deflagration, are the tangent points between the Rayleigh line and the Hugoniot curve relevant to $Q = E_0/2$. If we carry out our analysis for a generic $Q \geq 0$, the tangency condition reads

$$M_0^4 - 2\left(1 + \frac{16}{15}Q\right)M_0^2 + 1 = 0 \tag{36}$$

and yields for M_0^2 the values

$$M_L = 1 + \frac{16}{15}Q\left(1 - \sqrt{1 + \frac{15}{8Q}}\right) < 1 \tag{37}$$

for the lower C–J point and

$$M_U = 1 + \frac{16}{15}Q\left(1 + \sqrt{1 + \frac{15}{8Q}}\right) > 1 \tag{38}$$

for the upper C–J point on that general Hugoniot hyperbola. It is easy to see that tangency is impossible for $Q < 0$.

Clearly M_L and M_U evaluated at $Q = E_0/2$ coincide respectively with M_{eq}^- and M_{eq}^+, and we can underline that

$$M_{eq-} < M_L < M_U < M_{eq+}$$

for $Q < E_0/2$, and that existence condition for the two equilibria of the dynamical system coincides with intersection condition with the Rayleigh line for the hyperbola relevant to the burned state. We can also notice that the slope of the Hugoniot curve with $Q = 0$ at the unburned state is −5/3, so that the Rayleigh line is tangent to it when $M_0^2 = 1$. At $Q = 0$, the values of M_L and M_U coincide and are indeed equal to 1. As a final remark, let us note that condition for existence of equilibrium states $u_{eq}^{\pm}$ may be cast as $Q_s > E_0/2$, and

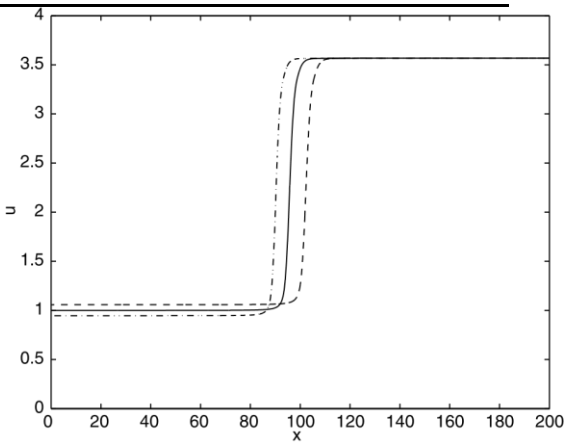

Fig. 1 On the choice of the flame eigenvalue for the considered deflagration. Behavior of velocity u for different values of μ: μ = 6208 (*solid line*), μ = 5700 (*dashed line*), μ = 6700 (*dash-dotted line*)

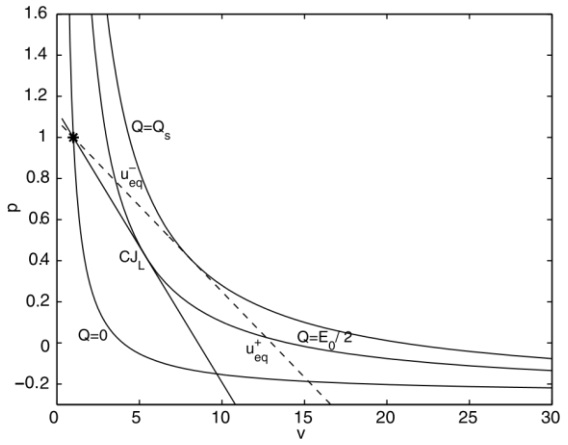

Fig. 2 Hugoniot curves and Rayleigh line on p versus v plane for the considered deflagration;

CJ_L denotes the lower Chapman–Jouguet point, '*' denotes the reference unburned state

little algebra shows that this is actually equivalent to $M_0^2 < M_{eq}^-$ or $M_0^2 > M_{eq}^+$. In case of equal sign ($Q_s = E_0/2$), the two equilibria coalesce in the unique value u_s. Similarly, the condition $Q < Q_s$ is equivalent to $M_0^2 < M_L$ or $M_0^2 > M_U$.

4 Detonation and Deflagration Profiles

As well known [12], due to the instability of all burned equilibrium states (the Jacobian has at least one positive eigenvalue), the numerical integration of the dynamical system (10) has to be performed backwards, starting from a neighborhood of the considered equilibrium point, and looking, by trial and error, for the possible phase trajectory leading eventually to the metastable unburned state (1,1,0), where the vector field of the dynamical system is almost zero if the (dimensionless) activation temperature threshold T_{act} is large enough, as assumed in these types of problems. For the sought steady wave to exist, it is then necessary that the unburned point belongs to the central (or stable, if applicable) manifold of the equilibrium

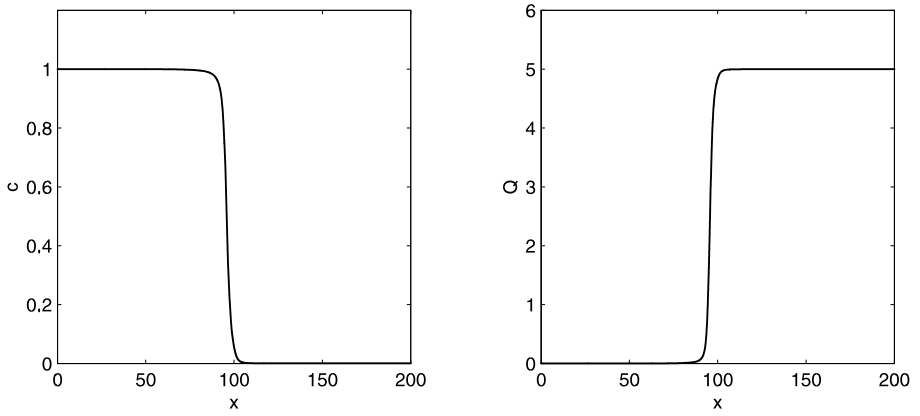

Fig. 3 Behavior of concentration c (*left*) and of the parameter Q(c,J,q) (*right*) in the considered weak deflagration process

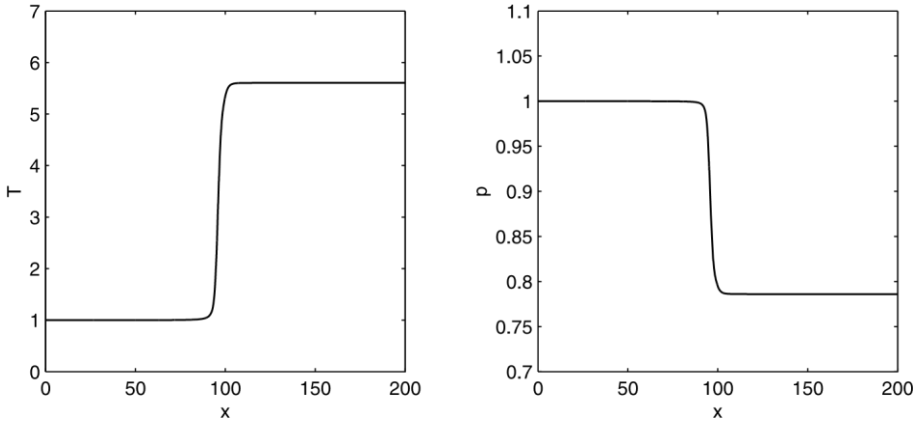

Fig. 4 Flame profile of temperature T (*left*) and scalar pressure p (*right*) versus x, in the considered weak deflagration process

point [10], a condition which implies a precise constraint on the physical parameters that characterize the process, and leads to the concept of flame eigenvalue, the control parameter μ already introduced in (14), which has to be determined once the other parameters are given. This constraint is the mathematical aspect of a well known physical problem [12], the precarious dependence of flames on the supply of fuel (namely on u_0 and T_0), once chemical reactivity k and thermal conductivity λ have been fixed. The flame eigenvalue is then searched for by a shooting method on the parameter μ. Once the steady solution (c,u,J) is determined, all physical quantities of interest, like n,T,q,ρ,p,v,Q, are known as functions of x, and also the Hugoniot diagram can be constructed. In this paper we shall confine ourselves to smooth (continuous) solutions. Treatment of jump discontinuity will hopefully be subject of future investigation.

We shall consider both deflagration and detonation waves, with typical values of dimensionless parameters such as L = 1, T_{act} = 25, E_0 = 10, for which M_1 = 0.0462,

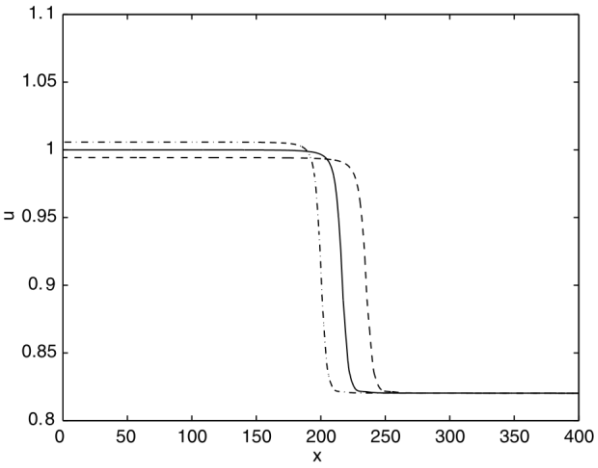

Fig. 5 On the choice of the flame eigenvalue for the considered detonation. Behavior of velocity u for different values of μ: μ = 20.95 (*solid line*), μ = 19 (*dashed line*), μ = 23 (*dash-dotted line*)

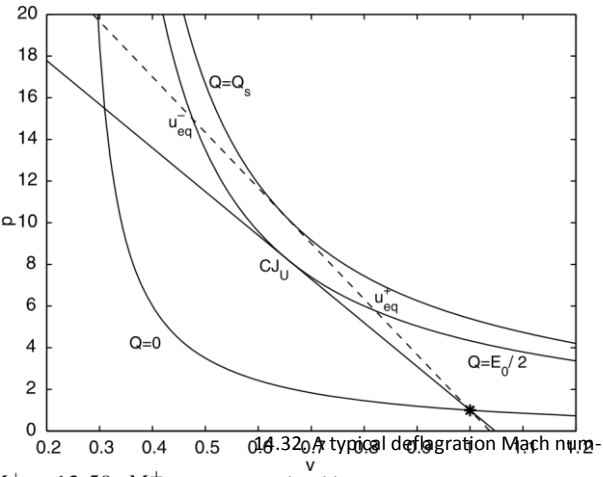

Fig. 6 Hugoniot curves and Rayleigh line on p versus v plane for the considered detonation; CJ_U denotes the upper Chapman–Jouguet point, '*' denotes the reference unburned state

M_2^- 14.32. A typical deflagration Mach number corresponds to M^2 $= 0.0754$, $M_{eq}^- = 0.0794$, $M_{eq}^+ = 12.59$, $M_2^+ =$ 0.05, and yields $_0 =$

$u^-_{eq} = 3.568$, $u^+_{eq} = 12.68$, $T_{eq}^- = 5.609$, $T_{eq}^+ = 0.6723$, $Q_s = 8.461$.

With this choice we are in the range 1(b) described in the deflagration Sect. 2.1, and we look for the smooth weak deflagration solution; the equilibrium $(0,u^-_{eq},0)$ exhibits a twodimensional unstable manifold and a one-dimensional central manifold (Figs. 1–4).

As regards the detonation regime, we choose a typical value such as $M_0^2 = 16$, and we obtain correspondingly

$u^-_{eq} = 0.4757$, $u^+_{eq} = 0.8212$, $T_{eq}^- = 14.25$, $T_{eq}^+ = 9.473$, $Q_s = 6.592$.

With this choice we are in the range 2 described in the detonation Sect. 2.2, and we search for the smooth weak detonation solution; the equilibrium $(0,u^+_{eq},0)$ exhibits a two-dimensional unstable manifold and a one-dimensional central manifold (Figs. 5–8).

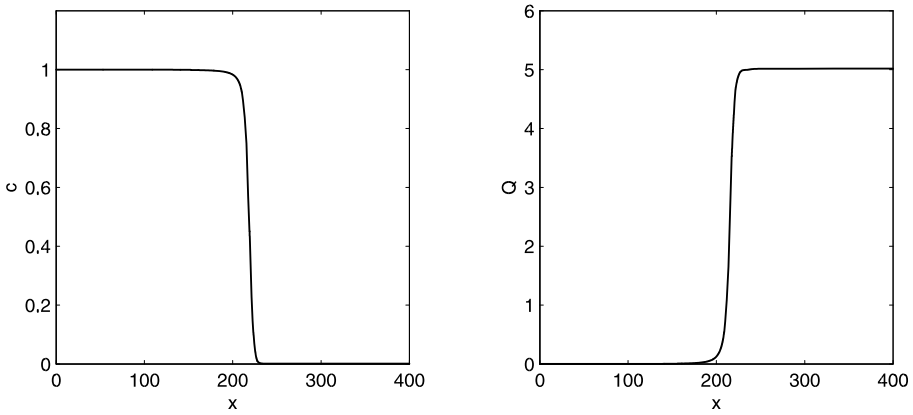

Fig. 7 Behavior of concentration c (*left*) and of the parameter Q(c,J,q) (*right*) in the considered weak detonation process

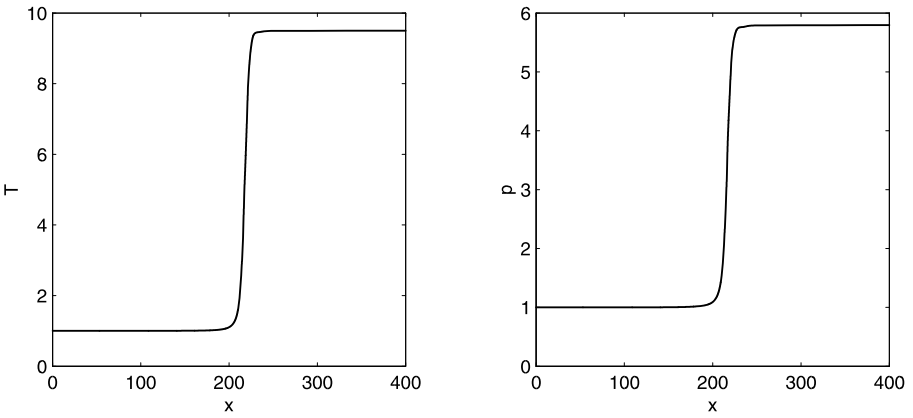

Fig. 8 Flame profile of temperature T (*left*) and scalar pressure p (*right*) versus x in the considered weak detonation process

Figures 1 and 5 illustrate the search for the flame eigenvalue, with reference to the state variable u, which coincides with the specific volume v. Values of μ slightly above or below the correct eigenvalue produce curves, not necessarily meaningful, which, in the backward integration, stabilize at velocities

which are different from the equilibrium values. As well known [11], deflagration corresponds to velocity increase across the wave front, and the opposite trend applies to detonation. One may notice that M_0^2 is two orders of magnitude higher for detonation than for deflagration, whereas the eigenvalue μ turns out to be two orders of magnitude smaller, in such a way that the products μM_0^2 are quite close. This implies by (14) that, for a given reaction with assigned microscopic reaction rate k and thermal conductivity λ, and with the gas inflow parameters u_0 and T_0 related by the given Mach number, the temperatures T_0 in the unburned states must be of the same order (though different from one another, of course) in the two steady processes (and thus very different values of u_0 are involved). In general, an extensive numerical campaign would be able to associate, for instance, to any k, λ, and T_0, the value of u_0 producing the sought steady combustion wave.

Figures 2 and 6 describe the Hugoniot diagram, showing the Rayleigh line (dashed line) and its interplay with the Hugoniot sheaf. In particular we plot here the hyperbolae characterized by Q = 0 (which the unburned state belongs to), Q = E_0/2 (which equilibrium burned states belong to), and Q = Q_s (tangent to the Rayleigh line). The lower and upper Chapman–Jouguet points are also given in the two cases of deflagration and detonation, respectively. Notice the different scales, dictated, for visibility reasons, by the very different values of M_0^2, which determine the very different slopes of the Rayleigh lines. Finally, Figs. 3, 4 and 6, 7 are a sample of the steady wave profiles for the most meaningful combustion quantities c,Q,T,ρ. The vertical scales are chosen to fit the actual values of the shown fields, the different horizontal scales are due again to the different values of M_0^2. On both scales the wave width is quite small, and the wave itself has been (conventionally) located in the middle of the range. One can observe that all state variables exhibit trends which are typical of either deflagration or detonation [11]. In particular, temperature is increasing in both processes, whereas pressure is very slightly decreasing for deflagration and considerably increasing for detonation, in agreement with the fact that the Rayleigh line is very flat or very steep, respectively. Moreover, the parameter Q is always monotonically increasing from 0 to E_0/2. In fact, Q increases with u (see (32)) and u increases with x (see Figs. 1 and 3 (right)) in the first (subsonic) case, whereas both trends are reversed in the latter, which is supersonic (see (32) and Figs. 5 and 7 (right)).

Acknowledgements This work was performed in the frame of the activities sponsored by GNFM–INdAM, and by the Universities of Messina, Parma, and Torino Politecnico.

References

1. Abramowitz, M., Stegun, I.A. (eds.): Handbook of Mathematical Functions. Dover, New York (1965)
2. Buckmaster, J.D. (ed.): The Mathematics of Combustion. SIAM, Philadelphia (1985)
3. Cercignani, C.: The Boltzmann Equation and Its Applications. Springer, New York (1988)
4. Chapman, S., Cowling, T.G.: The Mathematical Theory of Non-uniform Gases. University Press, Cambridge (1970)
5. Conforto, F., Groppi, M., Monaco, R., Spiga, G.: Kinetic approach to deflagration processes in a recombination reaction. Kinet. Relat. Models **4**, 259–276 (2011)
6. Fickett, W.: Introduction to Detonation Theory. University of California Press, Berkeley (1985)
7. Fickett, W., Davis, W.C.: Detonation, Theory and Experiment. Dover, New York (1979)
8. Glassman, I.: Combustion. Academic Press, New York (1987)
9. Groppi, M., Rossani, A., Spiga, G.: Kinetic theory of a diatomic gas with reactions of dissociation andrecombination through a transition state. J. Phys. A, Math. Gen. **33**, 8819–8833 (2000)
10. Guckenheimer, J., Holmes, P.: Nonlinear Oscillations, Dynamical Systems, and Bifurcations of VectorFields. Springer, New York (1983)
11. Kuo, K.K.: Principles of Combustion. Wiley, Hoboken (2005)
12. Müller, I.: Flame structure in ordinary and extended thermodynamics. In: Ruggeri, T., Sammartino, M.(eds.) Asymptotic Methods in Nonlinear Wave Phenomena, pp. 144–153. World Scientific, Singapore (2007)
13. Müller, I., Ruggeri, T.: Rational Extended Thermodynamics. Springer, New York (1998)

14. Takata, S.: Kinetic theory analysis of the two-surface problem of a vapor–vapor mixture in the continuumlimit. Phys. Fluids **16**, 2182–2198 (2004)
15. Takata, S., Aoki, K.: Two-surface problems of a multicomponent mixture of vapors and non condensablegases in the continuum limit in the light of kinetic theory. Phys. Fluids **11**, 2743–2756 (1999)